

naphthaleneethanol or cinnamyl alcohol was added to serve as a standard. The pH of the solution was adjusted to ca. 7, and it was then analyzed directly by HPLC on a Waters C18 Resolve Radial Pak column. The products were eluted with 55% methanol–45% water, 1.5 mL/min, and monitored by UV detection at 254 nm. The yields of tetraols were determined by comparing the areas of their HPLC peaks with the area of the peak due to the standard compound. It was assumed that the acid-catalyzed reactions of **DE-1** and **DE-2** at pH 4 yielded 100% tetraols, and the yields of tetraols from **DE-1** and **DE-2** under other conditions were determined relative to their yields at pH 4.

The azide adducts were analyzed with the same HPLC conditions used for analyzing tetraols, except for the solvent flow rate. The retention times (min) for the products from **DE-1**, with HPLC flow rate 3 mL/min, were as follows: tetraol from trans hydration, 5.4; tetraol from cis hydration, 10.1; azide adduct from cis addition, 20.9; azide adduct from trans addition, 26.1; 2-naphthaleneethanol (standard), 8.1. The retention times (min) for the products from **DE-2**, with HPLC flow rate 2.5 mL/min, were as follows: tetraol from trans hydration, 6.6; tetraol from cis hydration, 8.8; 2-naphthaleneethanol, 10.9; azide adduct(s), 16.2.

The *N*-acetylcysteine adducts from **DE-1** were analyzed by HPLC as described above, with 20% methanol–80% water as the eluent and a flow rate of 1.0 mL/min. The retention times (min) of the products were as follows: trans adduct from (–)-**DE-1**, 6.4; trans adduct from (+)-**DE-1**, 7.3; cis adduct from (–)-**DE-1**, 9.4; cis adduct from (+)-**DE-1**, 10.1.

Only two *N*-acetylcysteine adducts formed in equal amounts were detected from the reaction of racemic **DE-2** in solutions containing *N*-acetyl-L-cysteine at pH 8.5, and the HPLC retention times (min) of these adducts (20% methanol–80% water as eluent, 0.5 mL/min) were 13.1 and 15.5. The diastereomeric adducts presumably are formed from trans addition of the thiolate group to the (+) and (–) enantiomers of **DE-2**.

**Acknowledgment.** This investigation was supported by Public Health Service Grants Nos. CA-17278 and CA-26086 (D.L.W.) from the National Cancer Institute. Helpful discussions with Drs. Ralph Pollack (UMBC), Paul Dietze (UMBC), and Jane Sayer (National Institutes of Health) and comments from Dr. W. P. Jencks are greatly appreciated.

## Reagents and Methods for the Solid-Phase Synthesis of Protein–EDTA for Use in Affinity Cleaving

James P. Sluka, John H. Griffin, David P. Mack, and Peter B. Dervan\*

Contribution from the Arnold and Mabel Beckman Laboratories of Chemical Synthesis, California Institute of Technology, Pasadena, California 91125. Received February 5, 1990

**Abstract:** Synthetic procedures for the introduction of the metal chelator ethylenediaminetetraacetic acid (EDTA) at unique amino acid positions of proteins by solid-phase methods are described. Two protected derivatives of EDTA compatible with Merrifield solid-phase protein synthesis employing *N*-tert-butyloxycarbonyl- (Boc-) protected amino acids were developed. The first reagent is a dipeptide with three of four carboxyl groups of EDTA protected as benzyl esters and the fourth coupled to a  $\gamma$ -aminobutanoic acid linker, referred to as tribenzyl-EDTA–GABA (BEG). A second reagent is the tricyclohexyl ester of EDTA, TCE. BEG and TCE allow the modification of the NH<sub>2</sub> terminus and/or lysine side chains of resin-bound peptides and proteins. Upon deprotection and cleavage from the resin, a protein is produced with EDTA at a defined amino acid position. The availability of protein–EDTA conjugates extends the affinity cleaving method to the study of protein–DNA complexes in solution.

### Introduction

High-resolution crystallographic views of DNA binding proteins and protein–DNA complexes reveal the structural complexity of protein–DNA interactions.<sup>1–4</sup> The combination of direct protein–DNA contacts mediated by multiple hydrogen bonds and sequence-dependent DNA conformational effects limits our ability to make detailed structural predictions, even if a new DNA binding protein can be assigned to a structural class such as helix–turn–helix,<sup>1–3</sup> double-barreled helix,<sup>4</sup> zinc binding finger,<sup>5</sup> or scissor grip leucine zipper.<sup>6</sup> In the absence of high-resolution crystallographic and nuclear magnetic resonance data, solution methods, such as affinity cleaving, are needed to determine the topology of protein–DNA complexes and correlate sequence similarities with known structural classes.<sup>7–8</sup>

**Affinity Cleaving.** Attachment of EDTA·Fe to a DNA binding moiety creates a DNA cleaving molecule that functions under physiologically relevant pH, temperature, and salt conditions.<sup>9</sup> The cleavage reaction can be initiated by addition of a reducing agent such as dithiothreitol or sodium ascorbate.<sup>9</sup> If the DNA binding molecule is sequence specific, the EDTA·Fe cleaves at highly localized sites on DNA restriction fragments and plasmids.<sup>10–16</sup> Because the EDTA·Fe cleaving moiety is not sequence

(7) Most protein–DNA complexes characterized to date involve major groove contacts. Minor groove protein–DNA contacts conferring sequence-specific affinity are less well documented, although a few recent examples exist.<sup>8</sup>

(8) (a) Yang, C. C.; Nash, H. A. *Cell* **1989**, *57*, 869. (b) Suzuki, M. *EMBO J.* **1989**, *8*, 797.

(9) (a) Hertzberg, R. P.; Dervan, P. B. *J. Am. Chem. Soc.* **1982**, *104*, 313. (b) Hertzberg, R. P.; Dervan, P. B. *Biochemistry* **1984**, *23*, 3934.

(10) (a) Schultz, P. G.; Taylor, J. S.; Dervan, P. B. *J. Am. Chem. Soc.* **1982**, *104*, 6861. (b) Taylor, J. S.; Schultz, P. G.; Dervan, P. G. *Tetrahedron* **1984**, *40*, 457. (c) Schultz, P. B.; Dervan, P. B. *J. Am. Chem. Soc.* **1983**, *105*, 7748.

(11) Dervan, P. B. *Science* **1986**, *232*, 464.

(12) (a) Youngquist, R. S.; Dervan, P. B. *Proc. Natl. Acad. Sci. U.S.A.* **1985**, *82*, 2565. (b) Youngquist, R. S.; Dervan, P. B. *J. Am. Chem. Soc.* **1985**, *107*, 5528. (c) Griffin, J. H.; Dervan, P. B. *J. Am. Chem. Soc.* **1986**, *108*, 5008. (d) Sluka, J. P.; Dervan, P. B. In *New Synthetic Methodology and Functionally Interesting Compounds, Proceedings of the 3rd International Kyoto Conference on New Aspects of Organic Chemistry*; Yoshida, Z.-I., Ed.; Elsevier: New York, 1986; Vol. 25, pp 307–322. (e) Youngquist, R. S.; Dervan, P. B. *J. Am. Chem. Soc.* **1987**, *109*, 7564. (f) Wade, W. S.; Dervan, P. B. *J. Am. Chem. Soc.* **1987**, *109*, 1574. (g) Griffin, J. H.; Dervan, P. B. *J. Am. Chem. Soc.* **1987**, *109*, 6840.

(13) (a) Moser, H.; Dervan, P. B. *Science* **1987**, *238*, 645. (b) Griffin, L. C.; Dervan, P. B. *Science* **1989**, *245*, 967.

(1) (a) Aggarwal, A. K.; Rodgers, D. W.; Drottar, M.; Ptashne, M.; Harrison, S. C. *Science* **1988**, *242*, 899. (b) Anderson, J. E.; Ptashne, M.; Harrison, S. C. *Science* **1987**, *326*, 846.

(2) Otwinowski, Z.; Schevitz, R. W.; Zhang, R. G.; Lawson, C. L.; Joachimiak, A.; Marmorstein, R. Q.; Luisi, B. F.; Sigler, P. B. *Nature* **1988**, *335*, 321.

(3) Jordan, S. R.; Pabo, C. O. *Science* **1988**, *242*, 893.

(4) McClarin, J. A.; Frederick, C. A.; Wang, B. C.; Greene, P.; Boyer, H. W.; Grable, J.; Rosenberg, J. M. *Science* **1986**, *234*, 1526.

(5) (a) Miller, J.; McLachlan, A. D.; Klug, A. *EMBO J.* **1985**, *4*, 1609. (b) Berg, J. M. *Proc. Natl. Acad. Sci. U.S.A.* **1988**, *85*, 99. (c) Párraga, G.; Horvath, S. J.; Eisen, A.; Taylor, W. E.; Hood, L. E.; Young, E. T.; Klevit, R. E. *Science* **1988**, *241*, 1489. (d) Lea, M. S.; Gippert, G. P.; Saman, R. V.; Case, D. A.; Wright, P. *Science* **1989**, *245*, 635.

(6) (a) Landschulz, W. H.; Johnson, P. F.; McKnight, S. L. *Science* **1988**, *240*, 1759. (b) Vinson, C. R.; Sigler, P. B.; McKnight, S. L. *Science* **1989**, *246*, 911, and references cited there.

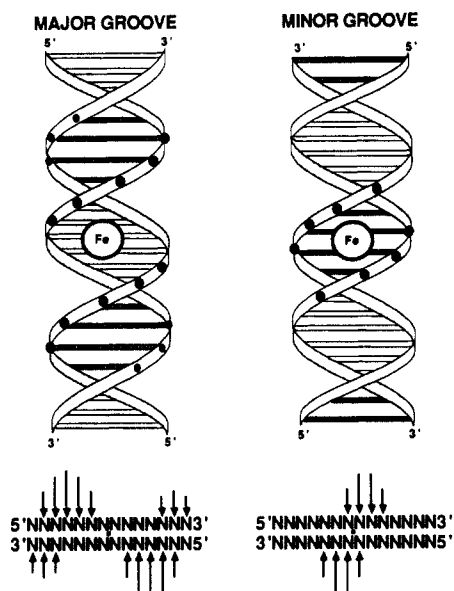


**Figure 1.** Cleavage pattern analysis. (Right) EDTA·Fe located in the minor groove generates an asymmetric cleavage pattern with maximal cleavage loci shifted to the 3'-side on opposite strands.<sup>10-13</sup> (Left) When the EDTA·Fe is located in the major groove, the maximal cleavage loci are 5'-shifted; in addition, cleavage of lower efficiency occurs on the distal strands of the adjacent minor grooves.<sup>13</sup> This results in an overall pattern of a pair of 3'-shifted asymmetric cleavage loci of unequal intensity on opposite strands.<sup>13</sup> These patterns can be explained if the diffusible radical generated from the localized EDTA·Fe reacts with the major and minor grooves of DNA with unequal rates and preferentially (though not necessarily exclusively) in the minor groove.<sup>17</sup> Filled circles represent points of cleavage along the phosphodiester backbone. Sizes of circles represent extent of cleavage.

specific, the cleavage specificity is determined only by the binding specificity of the molecule being investigated. EDTA·Fe-equipped DNA binding molecules cleave DNA by oxidation of the deoxyribose backbone via a diffusible oxidant, presumably hydroxyl radical.<sup>9-16</sup> Cleavage of both DNA strands is observed and typically extends over four to six base pairs.<sup>9-16</sup> Due to the right-handed nature of double-helical DNA, the groove in which the EDTA·Fe is located can be identified by cleavage pattern analysis (Figure 1).

Affinity cleaving has been used to study the sequence-specific recognition of double-helical DNA by naturally occurring DNA binding antibiotics,<sup>10,11</sup> peptide analogues that bind in the minor groove,<sup>12</sup> and oligonucleotide-directed recognition of the major groove by triple-strand formation.<sup>13</sup> From these studies, which involve less complicated DNA binding motifs, numerous cleavage patterns caused by a diffusible oxidant produced in either the minor or the major groove of duplex DNA have been analyzed.

(14) (a) Sluka, J. P.; Horvath, S. J.; Bruist, M. F.; Simon, M. I.; Dervan, P. B. *Science* **1987**, *238*, 1129. (b) Sluka, J. P.; Horvath, S. J.; Glasgow, A. C.; Simon, M. I.; Dervan, P. B. *Biochemistry* **1990**, *29*, 6551. (c) Mack, D.; Shin, J.; Sluka, J. P.; Griffin, J. H.; Simon, M. I.; Dervan, P. B. *Biochemistry* **1990**, *29*, 6561.

(15) Oakley, M. G.; Dervan, P. B. *Science* **1990**, *248*, 847.

(16) Graham, K.; Dervan, P. B. *J. Biol. Chem.*, in press.

(17) Several lines of evidence support this view. Tullius has shown that a sinusoidal cleavage pattern is obtained when a DNA is bound to a precipitate of calcium phosphate and allowed to react with EDTA·Fe, demonstrating that the two grooves have a different reactivity toward EDTA·Fe.<sup>18</sup> EDTA·Fe attached to minor groove binding molecules affords cleavage patterns with single 3' shifted asymmetric cleavage loci per EDTA·Fe position.<sup>10-12</sup> However, for the case where EDTA·Fe is bound in the major groove of DNA by oligonucleotide triple helix formation, cleavage occurs along both strands of the adjacent minor grooves to afford a pair of cleavage loci of unequal intensity.<sup>13</sup> Cleavage is more intense along the strands proximal to the EDTA·Fe than along the distal strands of the adjacent minor grooves.

(18) (a) Tullius, T. D.; Dombrowski, B. A. *Science* **1985**, *230*, 679. (b) Tullius, T. D.; Dombrowski, B. A. *Proc. Natl. Acad. Sci. U.S.A.* **1986**, *83*, 5469. (c) Tullius, T. D.; Dombrowski, B. A.; Churchhill, M.; Kam, L. *Methods Enzymol.* **1987**, *155*, 537.

(19) Merrifield, R. B. *Adv. Enzymol.* **1969**, *32*, 221.

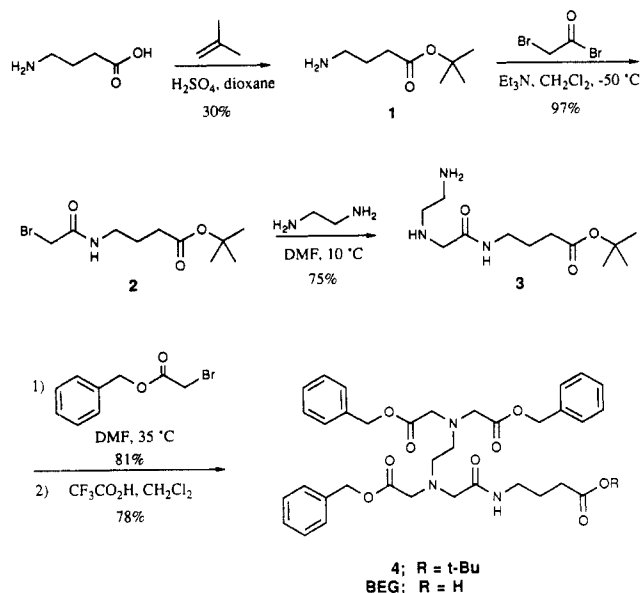


**Figure 2.** Synthesis of the tribenzyl ester of EDTA-GABA (BEG).

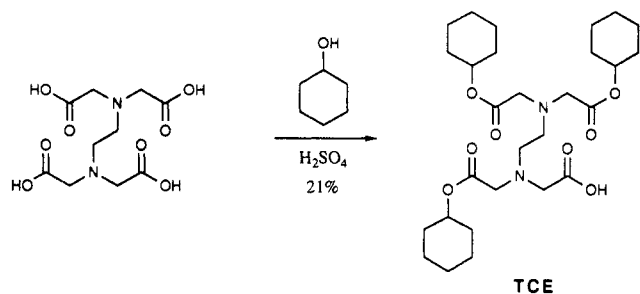


**Figure 3.** Synthesis of the tricyclohexyl ester of EDTA (TCE).

This data base allows interpretation of the affinity cleaving results from conformationally more complex proteins.<sup>14-16</sup>

**Characterization of Protein-DNA Structures by Affinity Cleaving.** Incorporation of EDTA·Fe at discrete amino acid residues within a protein allows the position and groove location of the modified residues to be mapped to nucleotide resolution.<sup>14-16</sup> The secondary and tertiary structures of DNA-protein complexes can be analyzed by affinity cleaving by use of two approaches. First, the amino acid location of the EDTA on a polypeptide chain of constant length may be varied in order to reveal key topological features of the protein-DNA complex (e.g., location of NH<sub>2</sub> versus COOH terminus).<sup>14-16</sup> Moreover, the length of the polypeptide may be incrementally changed while the EDTA is kept at the same terminus to examine the influence of substructures on the binding affinity of the protein and the conformational flexibility of a specific peptide fragment.<sup>14b,15</sup>

We describe here reagents and synthetic procedures for introducing a derivatized EDTA at unique amino acid positions of proteins by solid-phase methods (Figures 2 and 3). The availability of protein-EDTA conjugates has extended the affinity cleaving method to characterize the structural motifs of sequence-specific DNA binding proteins complexed with DNA in solution.

## Experimental Section

Proton nuclear magnetic resonance spectra were recorded at 400 MHz on a JEOL JNM GX400 and are reported in parts per million (ppm) downfield from Me<sub>4</sub>Si. Ultraviolet-visible spectra were recorded on a Perkin-Elmer Lambda 4C spectrophotometer. Infrared spectra were recorded on a Perkin-Elmer 1600 series FTIR. Mass spectra were recorded by using electron ionization (EI), chemical ionization (CI) or fast atom bombardment (FAB) techniques at the University of California, Riverside, or the Midwest Center for Mass Spectrometry at the University of Nebraska. All reagents were commercial grades and used without further purification unless noted. Ethylenediamine was distilled from sodium hydroxide under argon. Thin-layer chromatography (TLC)

was performed on EM Reagents silica gel plates (0.25  $\mu\text{m}$ ). Flash chromatography was performed using Merck silica gel (230–400 mesh).

**tert-Butyl  $\gamma$ -Aminobutanoate (1).** To a cold solution of concentrated sulfuric acid (20 mL) and dioxane (200 mL) in a 500-mL Parr bottle was added  $\gamma$ -aminobutanoic acid (12 g, 116 mmol). The mixture was cooled to  $-70^\circ\text{C}$  and isobutylene (100 mL) was condensed into the vessel. The bottle was stoppered and shaken at room temperature. After 6 h the bottle was cooled in ice and poured into a cold mixture of ethyl ether (500 mL) and 5 N sodium hydroxide (250 mL), and the organic layer was separated. The aqueous layer was extracted with ether ( $2 \times 200$  mL). The combined ether extracts were washed with 1 N sodium hydroxide ( $2 \times 200$  mL), dried ( $\text{Na}_2\text{SO}_4$ ), and concentrated under reduced pressure at  $35^\circ\text{C}$ . The crude product was distilled under vacuum at  $26\text{--}27^\circ\text{C}$  (0.04 mmHg) into a  $-70^\circ\text{C}$  trap affording 5.6 g (30%) of **1** as a colorless liquid:  $^1\text{H NMR}$  ( $\text{CDCl}_3$ )  $\delta$  2.72 (t, 2 H,  $J = 7.0$  Hz), 2.27 (t, 2 H,  $J = 7.0$  Hz), 1.73 (p, 2 H,  $J = 7.0$  Hz), 1.45 (s, 9 H), 1.14 (br s, 2 H) ppm; IR (film) 3382, 3302, 2977, 2932, 1728, 1367, 1158  $\text{cm}^{-1}$ ; HRMS (EI) for  $\text{C}_8\text{H}_{18}\text{NO}_2$  calcd 160.1337, found 160.1328.

**tert-Butyl *N*- $\delta$ -(Bromoacetamido)- $\gamma$ -aminobutanoate (2).** To a solution of bromoacetyl bromide (9.5 g, 47 mmol) in dichloromethane (175 mL) at  $-50^\circ\text{C}$  was slowly added a cold solution of triethylamine (5 g, 47 mmol), 4-(dimethylamino)pyridine (70 mg), and ester **1** (4.7 g, 30 mmol) in dichloromethane (50 mL). After 1 h at  $-50^\circ\text{C}$ , the flask and cooling bath were allowed to warm to room temperature over 2 h. The dichloromethane was removed under reduced pressure at  $25^\circ\text{C}$ . The resulting residue was taken up in ether (800 mL) and extracted with cold 0.1 N sodium hydroxide ( $2 \times 100$  mL), cold 0.1 N hydrochloric acid (100 mL), and cold water (50 mL). The ether extracts were dried ( $\text{MgSO}_4$ ) and concentrated to afford 8.1 g (97%) of crude bromoacetamide **2** as a light yellow liquid. Although the product can be purified by flash chromatography on silica gel (3%  $\text{CH}_3\text{OH}$  in  $\text{CH}_2\text{Cl}_2$ ), bromoacetamide **2** is unstable and was used in the next step without further purification:  $^1\text{H NMR}$  ( $\text{CDCl}_3$ )  $\delta$  6.8 (br s, 1 H), 3.88 (s, 2 H), 3.33 (q, 2 H,  $J = 6.6$  Hz), 2.23 (t, 2 H,  $J = 7.0$  Hz), 1.84 (p, 2 H,  $J = 7.0$  Hz), 1.46 (s, 9 H) ppm; IR (film) 3293, 3085, 2977, 2934, 1778, 1656, 1555, 1367, 1155  $\text{cm}^{-1}$ ; HRMS (CI) for  $\text{C}_{10}\text{H}_{19}\text{BrNO}_2$  calcd 280.0548, found 280.0544.

**tert-Butyl Ester Amine 3.** To freshly distilled ethylenediamine (27 mL) at  $10^\circ\text{C}$  was slowly added the crude bromoacetamide **2** (1.6 g, 5.8 mmol) in 2 mL of DMF. The solution was stirred for 1 h at  $10^\circ\text{C}$  and 2 h at room temperature. Solvent was removed under vacuum at  $25^\circ\text{C}$  and the crude product was purified by flash chromatography (5% concentrated  $\text{NH}_4\text{OH}$  in  $\text{CH}_3\text{OH}$ ) to afford 1.1 g (75%) of amine **3** as a yellow oil. *tert*-Butyl ester amine **3** is somewhat unstable and was used immediately:  $^1\text{H NMR}$  ( $\text{CDCl}_3$ )  $\delta$  7.27 (br s, 1 H), 3.30 (q, 2 H,  $J = 6.6$  Hz), 3.28 (s, 2 H), 2.82 (t, 2 H,  $J = 5.5$  Hz), 2.66 (t, 2 H,  $J = 5.5$  Hz), 2.27 (t, 2 H,  $J = 7.3$  Hz), 1.81 (p, 2 H,  $J = 7.3$  Hz), 1.68 (br s, 3 H), 1.46 (s, 9 H) ppm; IR (film) 3299, 3078, 2976, 2934, 1727, 1657, 1537, 1367, 1155  $\text{cm}^{-1}$ ; HRMS (CI) for  $\text{C}_{12}\text{H}_{26}\text{N}_3\text{O}_3$  calcd 260.1974, found 260.1958.

**tert-Butyl Ester of BEG (4).** To a solution of amine **3** (400 mg, 1.54 mmol) and diisopropylethylamine (632 mg, 4.90 mmol) in DMF (20 mL) was slowly added a solution of benzyl bromoacetate (1.18 g, 4.9 mmol) in DMF (10 mL). The mixture was stirred 1 h at room temperature and 15 h at  $35^\circ\text{C}$ . The DMF was removed under vacuum at  $35^\circ\text{C}$  and the crude product was dissolved in ether (100 mL), washed with water ( $3 \times 50$  mL) and saturated sodium chloride (50 mL), and dried ( $\text{Na}_2\text{SO}_4$ ). Concentration and flash chromatography (3%  $\text{CH}_3\text{OH}$  in  $\text{CH}_2\text{Cl}_2$ ) afforded 890 mg (81%) of *tert*-butyl ester **4** as a yellow oil:  $^1\text{H NMR}$  ( $\text{CDCl}_3$ )  $\delta$  8.07 (t, 1 H,  $J = 6.0$  Hz), 7.33 (m, 15 H), 5.11 (s, 6 H), 3.58 (s, 4 H), 3.40 (s, 2 H), 3.27 (s, 2 H), 3.23 (q, 2 H,  $J = 6.7$  Hz), 2.80 (t, 2 H,  $J = 5.1$  Hz), 2.75 (t, 2 H,  $J = 5.1$  Hz), 2.22 (t, 2 H,  $J = 7.5$  Hz), 1.76 (p, 2 H,  $J = 7.5$  Hz), 1.42 (s, 9 H) ppm; IR (film) 3315, 3064, 3034, 2971, 2932, 1741, 1728, 1668, 1528, 1455, 1367, 1175, 1151  $\text{cm}^{-1}$ ; HRMS (EI) for  $\text{C}_{39}\text{H}_{49}\text{N}_3\text{O}_9$  calcd 703.3469, found 703.3500. Anal. Calcd for  $\text{C}_{39}\text{H}_{49}\text{N}_3\text{O}_9$ : C, 66.57; H, 6.97; N, 5.97. Found: C, 66.77; H, 6.68; N, 6.04.

**BEG.** To a vigorously stirred solution of ester **4** (310 mg, 440  $\mu\text{mol}$ ) in dichloromethane (3 mL) was added trifluoroacetic acid (2 mL), and the resulting mixture was allowed to stir for 30 min at room temperature. The solvent was removed under reduced pressure at room temperature, and the residue was taken up in ethyl acetate (100 mL). The solution was washed with cold saturated sodium bicarbonate ( $2 \times 150$  mL) and saturated sodium chloride (150 mL) and dried ( $\text{Na}_2\text{SO}_4$ ). Concentration and flash chromatography (8%  $\text{CH}_3\text{OH}$  in  $\text{CH}_2\text{Cl}_2$  saturated with  $\text{H}_2\text{O}$ ) afforded BEG (230 mg, 78%) as a light yellow oil. BEG is unstable and should be stored frozen under argon:  $^1\text{H NMR}$  ( $\text{Me}_2\text{SO}-d_6 + \text{TFA}$ )  $\delta$  8.50 (t, 1 H,  $J = 6.0$  Hz), 7.37 (m, 15 H), 5.23 (s, 2 H), 5.12 (s, 4 H), 4.40 (s, 2 H), 4.08 (s, 2 H), 3.76 (s, 4 H), 3.39 (t, 2 H,  $J = 7.0$  Hz), 3.16 (m, 4 H), 2.26 (t, 2 H,  $J = 7.3$  Hz), 1.68 (p, 2 H,  $J = 7.1$  Hz) ppm; IR (film) 3274, 3065, 3033, 2956, 2856, 1738, 1732, 1668, 1633, 1542, 1455,

1185, 1141, 987  $\text{cm}^{-1}$ ; HRMS (FAB) for  $\text{C}_{35}\text{H}_{42}\text{N}_3\text{O}_9$  calcd 648.2920, found 648.2914. Anal. Calcd for  $\text{C}_{35}\text{H}_{42}\text{N}_3\text{O}_9$ : C, 64.91; H, 6.34; N, 6.49. Found: C, 64.94; H, 6.41; N, 6.42.

**TCE.** A stirred slurry of ethylenediaminetetraacetic acid (EDTA; 10 g, 34 mmol) in cyclohexanol (70 mL) containing concentrated sulfuric acid (2 mL) was heated at  $115^\circ\text{C}$  for 10 h, at which time nearly all of the EDTA had dissolved. The mixture was cooled to room temperature, poured into saturated aqueous sodium bicarbonate solution (500 mL), and extracted with ether ( $2 \times 200$  mL). The combined extracts were dried ( $\text{Na}_2\text{SO}_4$ ) and concentrated under reduced pressure and then in vacuo to afford a thick gum. The product was purified by flash chromatography (3%  $\text{CH}_3\text{OH}$  in  $\text{CH}_2\text{Cl}_2$  followed by 30%  $\text{CH}_3\text{OH}$  in  $\text{CH}_2\text{Cl}_2$ ) to afford TCE as a brittle foam (3.9 g, 21%):  $^1\text{H NMR}$  ( $\text{Me}_2\text{SO}-d_6$ )  $\delta$  4.68 (m, 3 H), 3.50 (s, 4 H), 3.49 (s, 2 H), 3.37 (s, 2 H), 2.71 (s, 4 H), 1.78–1.21 (m, 30 H) ppm; IR (film) 3448, 2937, 2858, 1735, 1634, 1452, 1198  $\text{cm}^{-1}$ ; HRMS (FAB) for  $\text{C}_{28}\text{H}_{46}\text{N}_2\text{O}_8$ , calcd 538.3240, found 538.3254. Anal. Calcd for  $\text{C}_{28}\text{H}_{46}\text{N}_2\text{O}_8$ : C, 62.43; H, 8.61; N, 5.20. Found: C, 62.31; H, 8.48; N, 5.11.

**Peptide Syntheses.** Peptides and proteins were prepared by employing *N*-*tert*-butyloxycarbonyl (Boc) amino acid derivatives for Merrifield solid-phase synthesis.<sup>19</sup> Manual peptide syntheses were carried out in 20-mL vessels fitted with a coarse glass frit as described by Kent.<sup>20a</sup> Automated syntheses were performed on an ABI 430A synthesizer,<sup>20</sup> modified by the removal of in-line filters to top and bottom of the reaction vessel, using a 20-mL Teflon/KelF reaction vessel.<sup>20</sup> The synthetic protocols used were developed at the California Institute of Technology.<sup>20</sup> Protected amino acid derivatives were purchased from Peninsula Laboratories. Boc-L-His (DNP) was obtained from Fluka. Asn-phenylacetamidomethyl (PAM) resin, dimethylformamide (DMF), diisopropylethylamine (DIEA), dicyclohexylcarbodiimide (DCC) in dichloromethane, *N*-hydroxybenzotriazole (HOBt) in DMF, and trifluoroacetic acid (TFA) were obtained from Applied Biosystems. Dichloromethane and methanol (HPLC grade) were purchased from Mallinckrodt, *p*-cresol and *p*-thiocresol from Aldrich, and diethyl ether (low peroxide content) from Baker.

*N*- $\alpha$ -Boc-L-amino acids were used with the following side chain protecting groups: Arg(Tos), Asp(OBzl), Glu(OBzl), His(DNP), Lys(Cl-Z), Ser(Bzl), Thr(Bzl), Trp(CHO), and Tyr(Br-Z). Manual assembly of the protected peptide on the solid support was carried out at  $25^\circ\text{C}$  using a three reaction step cycle. First the Boc protecting group was removed from the  $\alpha$ -amino group of the resin-bound amino acid with TFA (65% TFA in  $\text{CH}_2\text{Cl}_2$  for 1 and 15 min). The deprotected peptide resin was then neutralized with 10% DIEA in  $\text{CH}_2\text{Cl}_2$  ( $2 \times 1$  min). Amino acids (except Asn, Gln, and Arg) were coupled to the free  $\alpha$ -amino group as the symmetric anhydrides. For the first coupling, the symmetric anhydride was formed in situ in  $\text{CH}_2\text{Cl}_2$  by employing DCC. DMF was added after a sufficient activation time (10 min), and the reaction was allowed to proceed for a total of 30 min. Coupling yields were determined by quantitative ninhydrin monitoring<sup>21</sup> with acceptable values being  $\geq 99.7\%$  in the beginning of the synthesis and gradually decreasing to 99% near the end. If a second coupling was necessary, the resin was neutralized with 10% DIEA in DMF. The symmetric anhydride was formed outside the reaction vessel in a minimum of  $\text{CH}_2\text{Cl}_2$ . The solution was filtered into the vessel to remove the dicyclohexylurea and the vessel was filled with DMF. The reaction was allowed to proceed for 1 h. If the yield was not acceptable at this point, a third coupling was performed using the same protocol as the second coupling.

Asn, Gln, and Arg were coupled as the HOBt esters in DMF. The HOBt ester was formed in situ by combining the amino acid, DCC, and HOBt in DMF in the reaction vessel. Reaction times were longer due to the nature of the coupling reaction, typically 1–2 h. When second couplings were required for Asn and Gln, the same HOBt ester procedure was followed after neutralization with 10% DIEA in DMF. Second couplings for Arg were carried out using the preformed symmetric anhydride procedure above.

(20) (a) Kent, S. B. H. *Annu. Rev. Biochem.* **1988**, *57*, 957. (b) Kent, S. B. H.; Hood, L. E.; Beilan, H.; Meister, S.; Geiser, T. In *Peptides 1984: Proceedings of the 18th European Peptide Symposium, Sweden, 1984*; Ragnarsson, U., Ed.; Almquist & Wiksell: Stockholm, 1984; pp 185–188. (c) Kent, S. B. H.; Hood, L. E.; Beilan, H.; Bridgham, J.; Marriott, M.; Meister, S.; Geiser, T. In *Peptide Chemistry 1984, Proceedings of the Japanese Peptide Symposium*; Isumiya, N., Ed.; Protein Research Foundation: Osaka, 1985; pp 167–170. (d) Kent, S. B. H.; Clark-Lewis, I. In *Synthetic Peptides in Biology and Medicine*; Alitalo, K.; Partanen, P.; Vaheri, A., Eds.; Elsevier: Amsterdam, 1985; pp 29–57. (e) Kent, S. B. H.; Parker, K. F.; Schiller, D. L.; Wood, D. D.-L.; Clark-Lewis, I.; Chait, B. T. In *Peptides: Chemistry and Biology, Proceedings of the Tenth American Peptide Symposium*; Marshall, G. R., Ed.; ESCOM: Leiden, 1988; pp 173–178.

(21) Sarin, V. K.; Kent, S. B. H.; Tam, J. P.; Merrifield, R. B. *Anal. Biochem.* **1981**, *117*, 147.

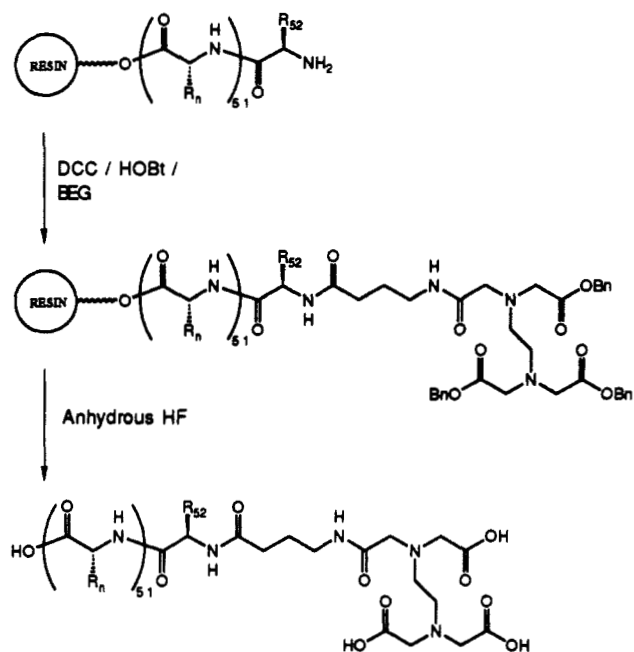


**Figure 4.** Synthetic scheme for the attachment and deprotection of BEG to the  $\text{NH}_2$  terminus of a protein using solid-phase methods.

**BEG and TCE Coupling to the  $\text{NH}_2$  Terminus of Resin-Bound Peptides (Figure 4).** A typical procedure for the coupling of BEG to the  $\text{NH}_2$  terminus of resin-bound peptide corresponding to the synthesis of EDTA-*Hin* (139-190),<sup>14a</sup> was as follows. A ~100-mg sample of peptide/resin (ca. 100  $\mu\text{mol/g}$ , total peptide ca. 10  $\mu\text{mol}$ ) was placed in a 12  $\times$  80 mm reactor, and the resin was swollen in  $\text{CH}_2\text{Cl}_2$  for 15 min. The resin was washed with  $\text{CH}_2\text{Cl}_2$  (5 $\times$ ), the terminal BOC protecting group removed, and the resin neutralized by standard procedures. BEG (125 mg, 194  $\mu\text{mol}$ ) and HOBt (50 mg, 330  $\mu\text{mol}$ ) were dissolved in DMF (2 mL) and DCC (42 mg, 203  $\mu\text{mol}$ ) was added. The solution was stirred 30 min at room temperature and added to the peptide/resin along with sufficient DMF to fill the reactor two-thirds full. Ninhydrin analysis indicated  $\geq 98\%$  reaction yield after 2-3 h. The peptide/resin was washed with DMF (4 $\times$ ) and  $\text{CH}_2\text{Cl}_2$  (4 $\times$ ). TCE was coupled to the  $\text{NH}_2$  terminus of resin-bound peptide, using the procedure described for BEG.

**TCE Coupling to the  $\epsilon$ - $\text{NH}_2$  Side Chain of a Lysine Residue (Figure 5).** *N*- $\alpha$ -Boc-*N*- $\epsilon$ -Fmoc-L-lysine (Chemical Dynamics Corp.) was coupled to the growing peptides as an HOBt ester by the standard procedure. The resin was washed with  $\text{CH}_2\text{Cl}_2$  (5 $\times$ ) followed by DMF (5 $\times$ ). The *N*- $\epsilon$ -Fmoc group was selectively removed by using 20% piperidine in DMF (a 1-min reaction step followed by a 10-min step) and the resin was washed with DMF (5 $\times$ ). TCE (1.08 g, 2 mmol, 4 equiv based on a 0.5-mmol synthesis) and HOBt (0.46 g, 3.4 mmol, 6.8 equiv) were dissolved in DMF (2 mL) and DCC (0.41 g, 2 mmol, 4 equiv) was added. The solution was stirred 30 min at room temperature and added to the peptide resin along with sufficient DMF to fill the reactor vessel two-thirds full. Ninhydrin analysis indicated 99.9% reaction after 1 h. The peptide resin was washed with DMF (5 $\times$ ) and  $\text{CH}_2\text{Cl}_2$  (5 $\times$ ). The *N*- $\alpha$ -Boc was removed as usual with TFA and the synthesis continued with the standard protocols.<sup>20</sup>

**Deprotection and Purification.** The histidine-protecting group, di-nitrophenyl (DNP), was removed at 25  $^\circ\text{C}$  by using 20% 2-mercaptoethanol and 10% DIEA in DMF; this treatment was repeated twice (2  $\times$  30 min). After removal of the *N*- $\alpha$ -Boc group with TFA and drying of the resin, all other side chain protecting groups as well as the peptide-resin bond were cleaved with anhydrous HF, in the presence of *p*-cresol and *p*-thiocresol as scavengers, for 60 min at 0  $^\circ\text{C}$ .<sup>20</sup> For peptides containing a Trp residue, the scavengers used were *p*-anisaldehyde and 1,4-butanedithiol. The HF was removed under vacuum. The crude protein was precipitated with diethyl ether, collected on a fritted funnel, dissolved in water, and filtered through, leaving the resin on the frit. A small sample was then removed, microfiltered, and subjected to analytical HPLC (Vydac 25 cm  $\times$  4.6 mm  $\text{C}_4$  column, 0-60% acetonitrile/0.1% TFA over 60 min). The remaining solution was frozen and lyophilized. Residual DNP groups were removed from the crude protein by treatment in 4 M guanidine hydrochloride, 50 mM Tris, pH 8.5, and 20% 2-mercaptoethanol for 1 h at 50  $^\circ\text{C}$ .<sup>20</sup> This solution was injected onto a semipreparative  $\text{C}_4$  HPLC column (25  $\times$  1 cm) and developed with  $\text{H}_2\text{O}/0.1\%$  TFA until the guanidine and 2-mercaptoethanol had eluted. A gradient of 0-60% acetonitrile/0.1% TFA was then run over 240 min.

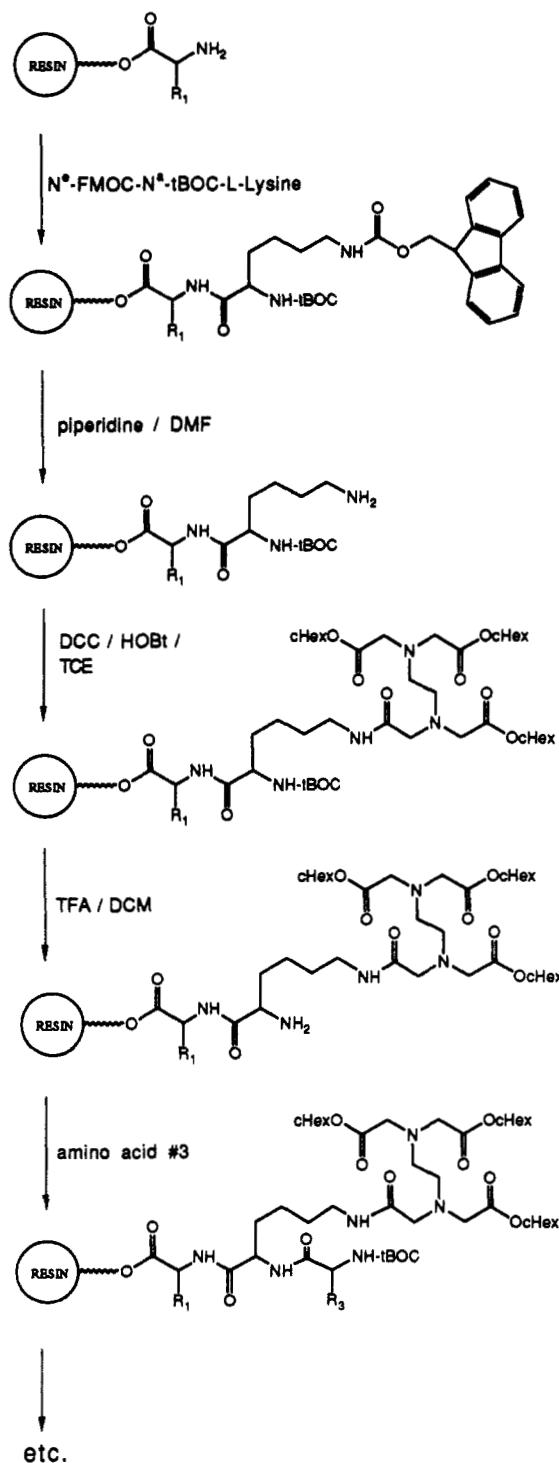


**Figure 5.** Synthetic scheme for the attachment of TCE to the  $\epsilon$ - $\text{NH}_2$  group of a lysine in the second amino acid position of a resin-bound peptide.

Fractions were collected and assayed for the presence of the desired protein by analytical HPLC. The protein concentrations were assayed based on calculated  $\text{OD}_{275}$  ( $\epsilon = 2800$  for two Tyr). Those fractions containing protein-EDTA were combined and lyophilized.

## Results and Discussion

Protecting groups for the EDTA carboxylic acids were chosen on the basis of standard side chain protection methods used for glutamic and aspartic acids in Merrifield solid-phase protein synthesis employing *N*-*tert*-butyloxycarbonyl (Boc) amino acid derivatives.<sup>19-22</sup> In BEG, three of the four carboxyl groups of EDTA are protected as benzyl esters. The fourth carboxyl is

(22) Tam, J. P.; Wong, T. W.; Riemen, M. W.; Tjoeny, F. S.; Merrifield, R. B. *Tetrahedron Lett.* 1979, 4033-4036.

coupled via an amide bond to a  $\gamma$ -aminobutanoic acid (GABA) linker designed to minimize disruptions of protein structure by the attached EDTA-Fe chelates (Figure 2). The protected dipeptide, tribenzyl-EDTA-GABA (BEG), was synthesized in four steps. Esterification of 4-aminobutanoic acid with isobutylene<sup>23</sup> produced the amino ester 1. Amidation of ester 1 with bromoacetyl bromide, followed by amination with excess ethylenediamine produced amine 3, containing the ethylenediamine core of EDTA with one carboxyl arm in place. Alkylation of amine 3 with 3 equiv of benzyl bromoacetate generated the *tert*-butyl ester 4. BEG was formed by deprotection of the *tert*-butyl ester 4 with trifluoroacetic acid in dichloromethane. The utility of BEG was demonstrated by the introduction of EDTA at the NH<sub>2</sub> terminus of the DNA binding domain from *Hin* recombinase, residues 139-190.<sup>14a</sup>

The tricyclohexyl ester of EDTA (TCE) has been developed as an alternative to BEG. TCE was synthesized in a single step by incomplete esterification of EDTA with cyclhexanol (Figure 3). TCE may be prepared on a larger scale than BEG, is more stable than BEG, and offers more flexibility than BEG in that a variety of amino acid linkers (or no linker at all) may be used. TCE, like BEG, couples with high efficiency to the NH<sub>2</sub> terminus or  $\epsilon$ -NH<sub>2</sub> group on the side chain of a lysine residue at the COOH terminus of resin-bound peptides (>98%) in the presence of DCC and HOBt in DMF.

For coupling BEG or TCE to the NH<sub>2</sub> terminus of resin-bound proteins, BEG or TCE was activated as an HOBt ester outside the reaction vessel by the addition of solid DCC and HOBt in a minimum of DMF for 30 min. The active ester was then added to the deprotected resin-bound protein and allowed to react for 2 h. Coupling was monitored by ninhydrin analysis, and the reaction was allowed to proceed for as long as necessary to achieve complete coupling (>98%). The crude EDTA-protein obtained after HF cleavage and deprotection was purified by reverse-phase HPLC. The presence of EDTA in such derivatives has been confirmed by <sup>1</sup>H NMR.<sup>24</sup>

For attachment of EDTA proximal to the COOH terminus of a resin-bound peptide, TCE was coupled to a lysine  $\epsilon$ -NH<sub>2</sub> side chain (Figure 5). This was accomplished by differential transient protection of the lysine NH<sub>2</sub> groups utilizing *N*- $\epsilon$ -Fmoc-*N*- $\alpha$ -Boc-L-lysine in the synthesis. Selective removal of the  $\epsilon$ -NH<sub>2</sub> protecting group was accomplished with piperidine for subsequent reaction with TCE.

Though BEG and TCE are formally amino acids, they are suitable only for capping an amino terminus or lysine side chain since they do not have a primary or secondary amino group for further chain extension. Current methodology only allows attachment of EDTA to the NH<sub>2</sub> residues of resin-bound protected peptides.<sup>25</sup> In addition, the approach of transient protection of the  $\epsilon$ -NH<sub>2</sub> side chain of lysine with Fmoc, for subsequent coupling

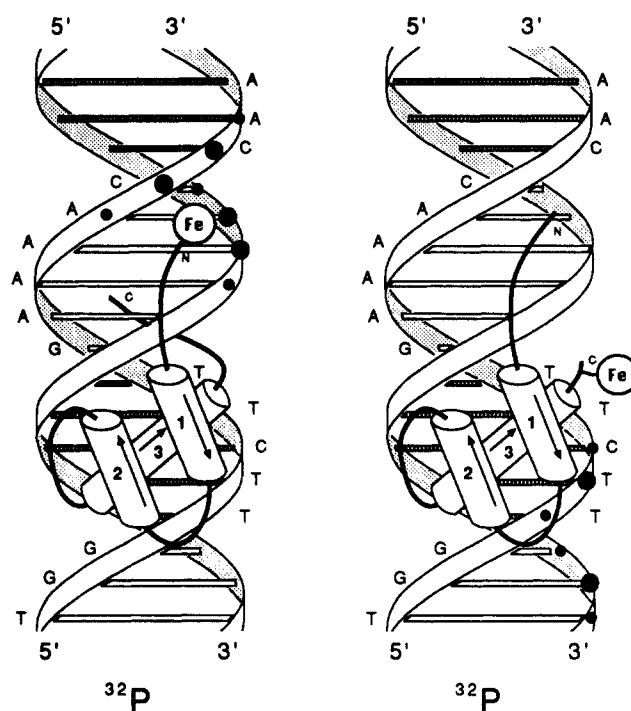


**Figure 6.** (Left) Fe-EDTA-*Hin*(139-190) mapping of the location of the NH<sub>2</sub> terminus of the DNA binding domain of *Hin* in the minor groove toward the symmetry axis site of the 13 bp *Hin* half-site.<sup>14a,b</sup> (Right) *Hin*(139-186)-EDTA-Fe maps the location of the COOH terminus of the DNA binding domain of *Hin* recombinase in the major groove. The putative recognition helix is oriented (N→C) toward the symmetry axis of the *Hin* binding site.<sup>14c</sup> Filled circles represent points of cleavage along the phosphodiester backbone. Sizes of circles represent extent of cleavage.

with TCE (or BEG) may be limited to the first few residues at the COOH terminus near the beginning of the peptide chain synthesis. EDTA modification of internal  $\epsilon$ -lysine side chains of peptides in the *t*-Boc-based synthesis has not yet been documented.<sup>25</sup> Thus, BEG and TCE represent only the first steps in the development of a class of modified amino acids compatible with Merrifield synthesis for the construction of hybrid proteins with novel functions.

**Applications to Protein-DNA Structures.** This methodology has been used to investigate the tertiary structures of the DNA binding domains of *Hin* recombinase and  $\gamma\delta$  resolvase, thought to bind DNA by a helix-turn-helix motif, as well as the DNA binding domain of the transcriptional activator GCN4 thought to bind DNA by the leucine zipper motif. A synthetic 52-residue protein based on the sequence-specific DNA binding domain of *Hin* recombinase (residues 139-190) with EDTA-Fe at the NH<sub>2</sub> terminus reveals that the NH<sub>2</sub> terminus of *Hin*(139-190) is bound in the minor groove of DNA near the symmetry axis of *Hin* binding sites.<sup>14</sup> A binding model put forward for *Hin*(139-190) includes a helix-turn-helix-turn-helix structure in the major groove with residues at the NH<sub>2</sub> terminus extending across the DNA phosphodiester backbone making specific contacts to the adjacent minor groove.<sup>14</sup> Attachment of EDTA-Fe to a lysine side chain (Ser<sup>183</sup>→Lys<sup>183</sup>) at the COOH terminus of *Hin*(139-184) reveals that the recognition helix is oriented toward the symmetry axis of the site (Figure 6).<sup>14</sup> From sequence comparisons, the DNA binding domain of  $\gamma\delta$  resolvase is also thought to bind DNA by a helix-turn-helix motif. Incorporation of EDTA-Fe at the NH<sub>2</sub> and COOH termini of  $\gamma\delta$ (141-183), respectively, reveals that the NH<sub>2</sub> terminus is bound in the minor groove of DNA near the symmetry axis of  $\gamma\delta$  binding sites similar to *Hin*(139-190).<sup>16</sup> Attachment of EDTA-Fe to a lysine side chain (Ser<sup>182</sup>→Lys<sup>182</sup>) at the COOH terminus of  $\gamma\delta$ (141-183) reveals that the recognition helix is oriented toward the symmetry axis of the site.<sup>16</sup> From analysis of the cleavage patterns of Fe-EDTA-GCN4(222-281), the NH<sub>2</sub> termini of a dimer of the DNA binding domain of the

(23) Roeske, R. *J. Org. Chem.* **1963**, *28*, 1251.

(24) Griffin, J. H. Ph.D. Thesis, California Institute of Technology, 1989.

(25) Other methods for the covalent attachment of metal chelators to proteins have employed the random reaction of electrophilic chelator derivatives with accessible nucleophilic sites such as lysyl  $\epsilon$ -amino groups found on the surfaces of proteins isolated from natural sources.<sup>26,27</sup> Recently, a 1,10-phenanthroline derivative was attached to available lysyl  $\epsilon$ -amines of the sequence-specific DNA binding Trp repressor protein.<sup>28</sup> In the presence of *l*-tryptophan, cupric ion, and 3-mercaptopropionic acid, the modified Trp repressor cleaved DNA at Trp binding sites. Analysis of 1,10-phenanthroline incorporation indicated that all four lysine residues of the Trp repressor had been modified. It was not possible to unambiguously identify which of the 1,10-phenanthroline-modified lysyl residue(s) were responsible for the DNA cleaving activity.

(26) Sundberg, M. W.; Meares, C. F.; Goodwin, D. A. *J. Med. Chem.* **1974**, *17*, 1304. (b) Yeh, S. M.; Sherman, D. G.; Meares, C. F. *Anal. Biochem.* **1979**, *100*, 152. (c) Meares, C. F.; McCall, M. J.; Reardan, D. T.; Goodwin, D. A.; Diamanti, C. I.; McTigue, M. *Anal. Biochem.* **1984**, *142*, 68.

(27) (a) Khaw, B. A.; Fallon, J. T.; Strauss, H. W.; Haber, E. *Science* **1980**, *209*, 295. (b) Scheinberg, D. A.; Strand, M.; Gansow, O. A. *Science* **1982**, *215*, 1511. (c) Rainsbury, R. M.; Westwood, J. H.; Coombes, R. C.; Neville, A. H.; Ott, R. J.; Kalirai, T. S.; McCready, V. R.; Gazet, J.-C. *Lancet* **1977**, *77*, 581. (d) Krecjcarek, G.; Tucker, K. *Biochem. Biophys. Res. Commun.* **1977**, *77*, 581.

(28) Chen, C. B.; Sigman, D. S. *Science* **1987**, *237*, 1197.

yeast transcriptional activator are located in the major groove nine to ten base pairs apart, symmetrically displaced four to five base pairs from the central C of the recognition site.<sup>15</sup> This provides experimental validation of the Y-shaped model recently put forward for a class of DNA binding proteins important in the regulation of gene expression.<sup>6k</sup>

**Summary.** We have designed and synthesized two peptide reagents, BEG and TCE, for the introduction of the metal chelator EDTA at discrete amino acid residues of peptides and proteins by Merrifield solid-phase protein synthesis employing Boc amino acids. Due to the ease of synthesis, stability, coupling efficiency, and flexibility in choice of linker, TCE is likely the reagent for most applications. These reagents have been used to attach EDTA to three different DNA binding domains, which has allowed the tertiary structures of the protein-DNA complexes to be characterized by affinity cleaving.<sup>14-16</sup> This information will contribute

to the body of knowledge necessary to define the principles for relating primary amino acid sequence to the tertiary structures of proteins bound to DNA and RNA. Moreover, because the reactive oxidant generated from EDTA-Fe can cause cleavage of proteins,<sup>29</sup> protein-EDTA-Fe molecules can be used for affinity cleaving studies of protein structure and protein-protein complexes.<sup>30</sup>

**Acknowledgment.** We are grateful for generous support from the DARPA University Research Initiative Program, Merck, an NSF predoctoral fellowship to J.H.G., and NIH traineeships to J.P.S. and D.P.M.

(29) Kim, K.; Rhee, S. G.; Stadtman, E. R. *J. Biol. Chem.* **1985**, *260*, 15394.

(30) Rana, T. M.; Meares, C. F. *J. Am. Chem. Soc.* **1990**, *112*, 2457.

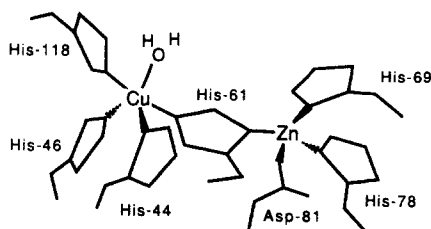
## NMR Studies of Nickel(II)-Substituted Derivatives of Bovine Copper-Zinc Superoxide Dismutase with Nickel(II) Bound in the Copper Site<sup>†</sup>

Li-June Ming and Joan Selverstone Valentine\*

Contribution from the Department of Chemistry and Biochemistry, University of California, Los Angeles, Los Angeles, California 90024. Received October 10, 1989

**Abstract:** Two new Ni<sup>2+</sup>-substituted derivatives of bovine copper-zinc superoxide dismutase (Cu<sub>2</sub>Zn<sub>2</sub>SOD) with Ni<sup>2+</sup> bound in the copper site have been prepared and studied by electronic and NMR spectroscopies. The Ni<sup>2+</sup> binding environment of these derivatives is found to be very similar to that of Cu<sup>2+</sup> in native SOD; i.e., the metal ion was coordinated to two histidines (presumably His-46 and His-118) through the N<sub>2</sub> nitrogen and to another histidine (presumably His-44) through the N<sub>δ1</sub> nitrogen as well as to the bridging His-61, which remained bridging even in the presence of anions. The anion binding properties of Ni<sup>2+</sup> were also found to resemble those of Cu<sup>2+</sup> in that site. Both azide and cyanide were found to bind to these Ni<sup>2+</sup>-substituted derivatives forming an axially symmetric metal binding site. Azide binding to the derivatives caused all the isotropically shifted signals to shift. However, all of the signals were still isotropically shifted out of the diamagnetic region in the presence of a saturating amount of azide, indicating that none of the coordinated histidines was completely detached from the metal coordination sphere under these conditions. Cyanide binding to these derivatives caused Ni<sup>2+</sup> to become diamagnetic, as shown by the disappearance of all the isotropically shifted <sup>1</sup>H NMR signals of the coordinated histidines. This observation leads us to the conclusion that the Ni<sup>2+</sup> becomes square planar upon cyanide binding, a result similar to that observed for native SOD studied by several different spectroscopic methods, e.g., EPR and EXAFS. The change of the spin state of Ni<sup>2+</sup> in these derivatives upon cyanide binding was also demonstrated by <sup>13</sup>C NMR spectroscopy using <sup>13</sup>CN<sup>-</sup>. Phosphate, however, did not perturb the Ni<sup>2+</sup> in the copper site significantly, suggesting its possible binding to positively charged residues near the metal binding site similar to its interaction with the native enzyme. The similarities of the structure of the Ni<sup>2+</sup> binding site in these derivatives and their anion adducts to those of the native SOD indicate that these derivatives can serve as good structural models for copper-zinc superoxide dismutase.

Copper-zinc superoxide dismutase (Cu<sub>2</sub>Zn<sub>2</sub>SOD)<sup>1</sup> isolated from bovine liver is a dimeric metalloprotein of molecular weight 31 200, containing a Cu<sup>2+</sup> and a Zn<sup>2+</sup> ion in each of its identical subunits bridged by the imidazole side chain of the histidine-61 residue.<sup>2</sup>



Much information concerning the nature of the metal binding sites, including geometries and configurations, anion interactions,

and SOD activity, has been obtained from examination of the properties of derivatives in which spectroscopically interesting metal ions have been substituted for the native metal ions.<sup>3</sup> Ni<sup>2+</sup> and Co<sup>2+</sup> substitution for Zn<sup>2+</sup> in bovine Cu<sub>2</sub>Zn<sub>2</sub>SOD has provided derivatives (i.e., Cu<sub>2</sub>Ni<sub>2</sub>SOD<sup>4</sup> and Cu<sub>2</sub>Co<sub>2</sub>SOD<sup>5</sup>) with high SOD activity, suggesting that these derivatives are good models for Cu<sub>2</sub>Zn<sub>2</sub>SOD. Because of the existence of magnetic coupling between Cu<sup>2+</sup> in the copper site and Ni<sup>2+</sup> or Co<sup>2+</sup> in the zinc site,

(1) Abbreviations: M<sub>2</sub>M'<sub>2</sub>SOD, M- and M'-substituted superoxide dismutase with M in the copper site and M' in the zinc site (an E in the above derivatives represents an empty site); EXAFS, extended X-ray absorption fine structure; ENDOR, electron nuclear double resonance; EPR, electron paramagnetic resonance; NMR, nuclear magnetic resonance; DEFT, driven equilibrium Fourier transform; FID, free induction decay.

(2) Tainer, J. A.; Getzoff, E. D.; Beem, K. M.; Richardson, J. S.; Richardson, D. C. *J. Mol. Biol.* **1982**, *160*, 181-217.

(3) Valentine, J. S.; Pantoliano, M. W. In *Copper Proteins*; Spiro, T. G., Ed.; Wiley: New York, 1981; Chapter 8.

(4) Ming, L.-J.; Valentine, J. S. *J. Am. Chem. Soc.* **1987**, *109*, 4426-4428.

(5) Fee, J. A. *J. Biol. Chem.* **1973**, *248*, 4229-4234.

<sup>†</sup> Presented in part at the XIII International Conference on Magnetic Resonance in Biological Systems, Madison, WI, August 14-19, 1988.